

# Improving Superheated Steam Temperature Control Using United Long Short-Term Memory and MPC

Qianchao Wang\*. Lei Pan\*. Kwang\_Y\_Lee\*\*.

\*Key Laboratory of Energy Thermal Conversion and Control of Ministry of Education,  
School of Energy and Environment, Southeast University, Nanjing, China  
(Tel: +86-25-83795951; email: 1692281094@qq.com; [panlei@seu.edu.cn](mailto:panlei@seu.edu.cn);  
Corresponding author [panlei@seu.edu.cn](mailto:panlei@seu.edu.cn))

\*\* Department of Electrical & Computer Engineering, Baylor University, Waco, TX 76798-7356, USA  
(e-mail: [Kwang\\_Y\\_Lee@baylor.edu](mailto:Kwang_Y_Lee@baylor.edu))

---

**Abstract:** Superheated steam temperature is one of the most important process variables for controlling the steam quality of thermal power units. In order to improve the accuracy of superheated steam temperature and the stability of valves for desuperheating water, this paper proposed a novel control strategy called united long short-term memory (LSTM) and model predictive control (MPC), which is weighted by particle swarm optimization. First, a deeply learnt inverse model is made to express the potential nonlinear dynamic characteristics of data and to predict the future valve opening in short-term. Secondly, model predictive control is used to control the secondary superheated steam temperature. Thirdly, the two predicted valve opening are weighted by particle swarm optimization. The combined deep learning inverse model control and MPC can make up the deficiencies of each other, i.e., over fitting of deep learning inverse model and linearity of MPC. The simulation experiments proved the advantage of LSTM-MPC in comparison with traditional PID and single MPC control.

*Keywords:* long short-term memory, model predictive control, particle swarm optimization, superheated steam temperature

---

## 1. INTRODUCTION

In order to improve the flexibility of thermal power unit operation, it is necessary to improve the control performance of the unit, the effect of superheated steam temperature on unit efficiency, and the safety during fast load tracking. Superheated steam temperature is usually associated with the change of steam flow, the heat change of flue gas and flow change of desuperheating water which make it too cumbersome and complicated to build a nonlinear model. Also, the calculation speed is too slow for most of the current superheated steam models. Therefore, we use linear models to approximate actual nonlinear models.

Because neural networks can theoretically approximate any characteristics of nonlinear models, it has been widely used in various applications. Intelligent algorithms such as long short-term memory, support vector machine, and deep belief network, etc. have been applied to predictive control or predictive modeling. EDM-LSTM algorithm (Ren, 2019) was used to predict short-term electrical load; A prediction model (Geng, 2019) was proposed for the state of charge of lithium-ion battery based on LSTM principle; Deep belief network and linear support vector machine (Chen, 2019) were combined to diagnose the fault of wind turbine pitch system.

For the superheated steam model, this paper proposed a novel control strategy called the united long short-term

memory and model predictive control (LSTM-MPC), consisting of the deep-learning inverse model control and model predictive control. First, a kind of recurrent neural network which is called long short-term memory is used to deeply learn the potential nonlinear dynamic characteristics of the secondary superheated steam temperature from field data for an inverse-model control. Secondly, an MPC with discrete model is established for the control on the secondary superheated steam temperature. Thirdly, the MPC and the LSTM are weighted, and the particle swarm optimization algorithm (PSO) is used to optimize the weights. The proposed LSTM-MPC control strategy not only solves the over-fitting problem that may exist in the neural network prediction model, but also reduces the fluctuation of the controlled variables which is predicted by MPC. Besides that, through modeling more nonlinear characteristics in the control strategy, it produces more appropriate control actions while the computation load decreases.

The rest of the paper is organized as follows. In Section 2, the secondary superheated steam temperature control system of a power plant in Nanjing is introduced. In Section 3, the LSTM-MPC is introduced. In Section 4, the advantages of LSTM-MPC is analyzed, and conclusion is drawn in Section 5.

## 2. AN OVERVIEW OF SUPERHEATED STEAM TEMPERATURE SYSTEM

The secondary superheated steam is in the last stage of the steam-water process. The schematic diagram of the secondary superheated steam temperature control of a power plant in Nanjing is shown in Fig. 1. The secondary superheated steam temperature control has two desuperheaters and one superheater and uses cascade PID control. The steam is desuperheated by the desuperheating water to bring the temperature to  $\theta_1$  and  $\theta_2$ . And then it is heated by the secondary superheater to reach the temperature  $\theta_3$ . Because desuperheating water is used to control superheated steam temperature, the whole system

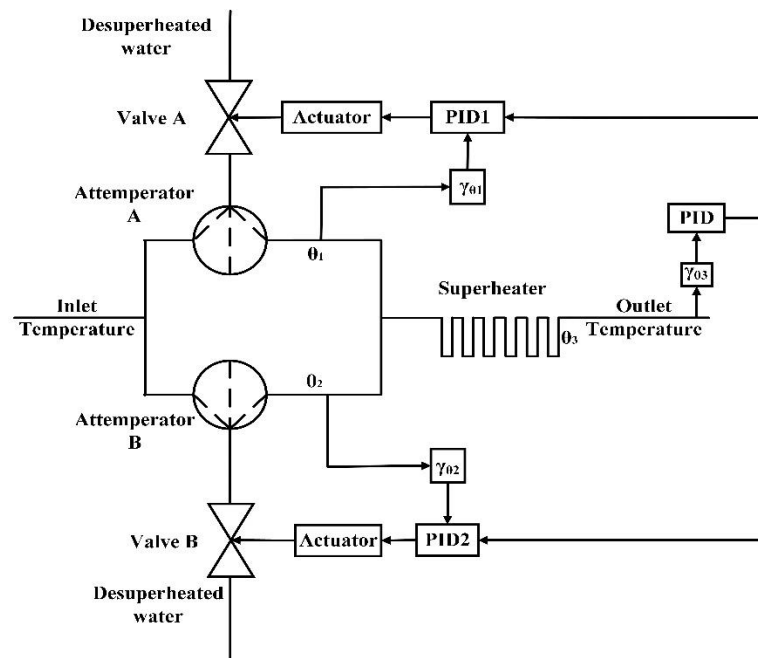


Fig. 1. The schematic diagram of the secondary superheated steam temperature control.

### 3. LSTM-MPC OF SUPERHEATED STEAM TEMPERATURE SYSTEM

The conventional PID control structure is simple, and easy to implement. However, it is difficult for conventional PID to overcome the characteristics of secondary superheated steam. Based on the identified linear discrete model, this paper proposes a control strategy (LSTM-MPC), combined by LSTM and MPC and weighted by PSO, which can effectively control the superheated steam and provide the stability of the desuperheating water valve.

#### 3.1 Model Predictive Control

Model predictive control is a model-based control algorithm. It was proposed for linear or quasi-linear system control in the early days and has been widely used in the process industry. The MPC includes prediction model, rolling optimization and feedback correction and uses the prediction model to predict the future output of the system. It has good ability to solve optimal control problem with constraints for large inertia and multi-

has characteristics such as large delay, time-varying, and nonlinearity. Furthermore, the water leakage of the valve at A side is terrible which is opposite to the valve at B side.

In desuperheater, the input variables are the inlet steam temperature of desuperheater, total steam flow and desuperheating water valve opening. The outlet steam temperature of desuperheater is the output variable. In the secondary superheater, the input variables are the inlet temperature of secondary superheater of A and B and steam flow of A and B. The outlet temperature of secondary superheater is the output variable.

variable processes. The basic control structure of MPC is shown in Fig. 2.

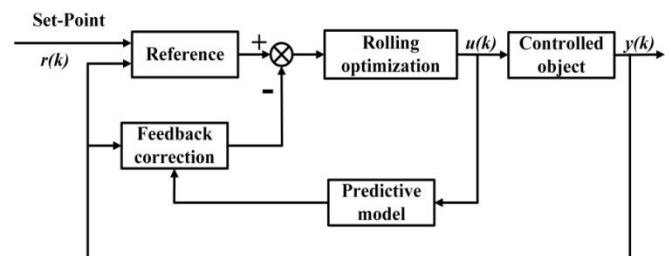


Fig. 2. The basic control structure of MPC.

In Fig. 2,  $r(k)$  is set-point of output of the system,  $u(k)$  is the input of the system, and  $y(k)$  is the actual output of the system. In the use of MPC, the prediction horizon  $P$ , control horizon  $M$ , constraints and optimization objective functions should be set appropriately.

The canonical MPC algorithm is weak at dealing with nonlinear dynamics and unknown disturbances. With some improvements on the algorithm, it can be used for optimization problems with uncertain factors (Xi, 2016),

and can achieve strong anti-interference ability (Cao, 2019) and robustness (Xiao, Fei, and Li, 2016). In this paper, a collaboration with neural network and deep learning is proposed to improve the MPC for controlling the plant with strong nonlinearity and unknown disturbances.

### 3.2 Long Short-Term Memory

The recurrent neural network (RNN) is proposed to solve the long-term dependence problem of sequence data. It can use the previous information for the current calculation and has the ability to approximate any nonlinearity theoretically. The structure of traditional RNN is shown in Fig. 3.  $x_i$  is the input at time  $i$ ;  $h_i$  is the output at time  $i$ .

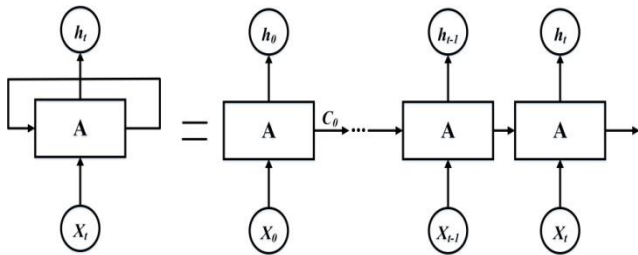


Fig. 3. The structure of RNN.

It can be seen from Fig. 3 that the input of the hidden layer A includes the outputs of the input layer and the hidden layer at the last time step. It means that the current and previous results can affect the hidden layer and the output of next time step by step. With the increase of numbers of hidden layers, RNN can learn the characteristics of data deeply and predict the short-term future output.

However traditional RNN encounters the gradient vanishing and the explosion (Rao, Huang, and Feng, 2018), so long short-term memory (LSTM) arises. As an improved RNN model, LSTM can learn long-term dependent information. Its network structure is similar to traditional recurrent neural network structure. Compared with the traditional RNN structure, LSTM introduces the concept of gate which is the key of it. The gate is used to control the disturbance of new information to the saved information of neural modules, so as to save the information for a long time. The neural module of LSTM is shown in Fig. 4.

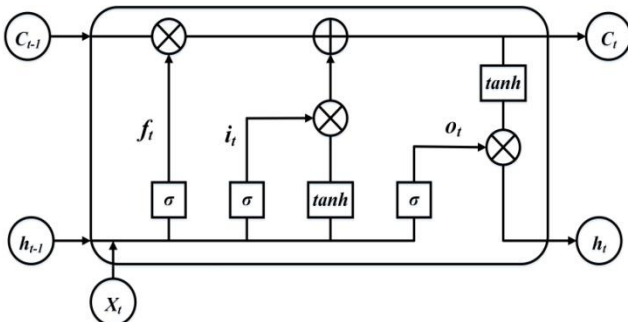


Fig. 4. The neural module of LSTM.

The input data of the LSTM module is composed of the unit state  $C_{t-1}$  transmitted from time  $t-1$  and the output  $h_{t-1}$  and the input  $X_t$  at time  $t$ . The output data are the unit state  $C_t$  and the output  $h_t$  at time  $t$ .

Each neural module contains three kinds of gate structures: forgetting gate  $f_t$ , input gate  $i_t$  and output gate  $o_t$ . The forgetting gate  $f_t$  determines the degree of influence of  $C_{t-1}$  on  $C_t$ , the input gate  $i_t$  determines how much input  $X_t$  is reserved to enter  $C_t$ , and the output gate  $o_t$  determines how much state unit  $C_t$  remains in the output  $h_t$ . Then  $C_t$  and  $h_t$  are involved in the calculation of LSTM at time  $t+1$ .

The specific calculation process of LSTM is as follows (1-5):

Calculation of forgetting gate  $f_t$ :

$$f_t = \text{sigmoid}(W_f \cdot [h_{t-1}, x_t] + b_f) \quad (1)$$

Calculation of input gate  $i_t$ :

$$i_t = \text{sigmoid}(W_i \cdot [h_{t-1}, x_t] + b_i) \quad (2)$$

Calculation of unit state:

$$c_t = f_t \circ c_{t-1} + i_t \circ \tanh(W_c \cdot [h_{t-1}, x_t] + b_c) \quad (3)$$

Calculation of output gate  $o_t$ :

$$o_t = \text{sigmoid}(W_o \cdot [h_{t-1}, x_t] + b_o) \quad (4)$$

Calculation of output:

$$h_t = o_t \circ \tanh(c_t) \quad (5)$$

Where  $f_t$  is the output of forgetting gate at time  $t$ ;  $i_t$  is the output of input gate at time  $t$ ;  $o_t$  is the output of output gate at time  $t$ ;  $W$  is the weight and  $b$  is the bias of the three gates.

*Sigmoid* and *tanh* are two activation functions, as shown in the formula (6-7):

$$\text{sigmoid}(x) = \frac{1}{1 + e^{-x}} \quad (6)$$

$$\text{tanh}(x) = \frac{e^x - e^{-x}}{e^x + e^{-x}} \quad (7)$$

Finally, the descending gradient method is used to get the optimal weight, so that the training result is close to the real result.

### 3.3 LSTM-MPC

In order to fully learn the potential nonlinearity and time-varying features in the data, this paper uses field data to train the recurrent neural network for approximating the actual plant. And then MPC based on the identified discrete model is incorporated into the control strategy for predicting the future inputs. The structure of LSTM-MPC is shown in Fig. 5.

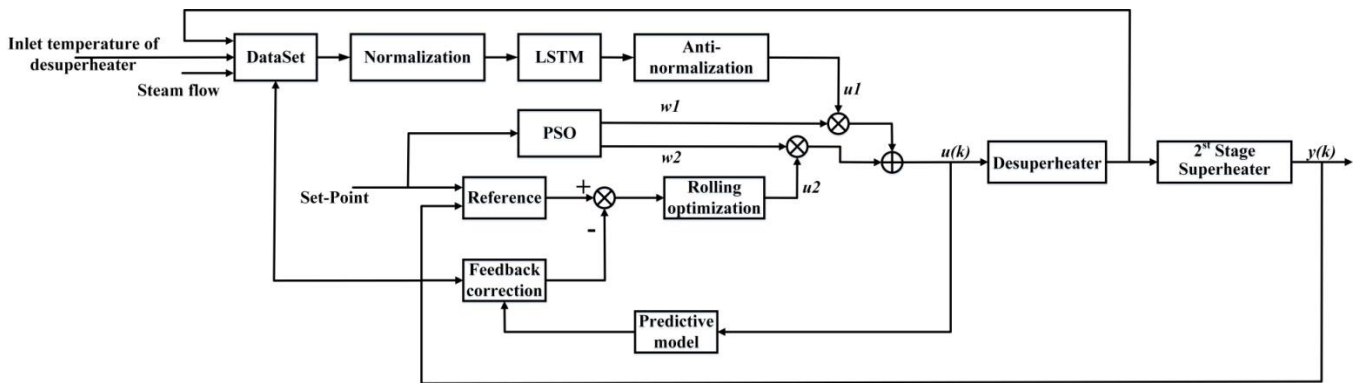


Fig. 5. The structure of LSTM-MPC.

### 3.3.1 LSTM Training

As shown in the structure diagram, the LSTM-MPC needs to train the valve opening of the desuperheater. So we need to establish an inverse model of valve opening. We built a deep RNN with four layers for the inverse model, and the LSTM is adopted for the inner two hidden layers, as shown in Fig. 6.

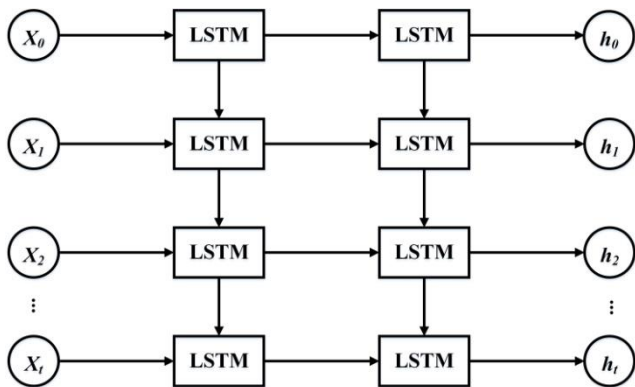


Fig. 6. The structure of deep RNN.

where  $X_i$  is the input at time  $i$ ;  $h_i$  is the output at time  $i$ .

Firstly, we need to choose related variables including inlet steam temperature of desuperheater, the total steam flow, outlet steam temperature of desuperheater and outlet temperature of secondary superheater as the inputs, and valve opening of the desuperheating water valve as the output. They form a variable set, with 17600 groups of field data. The first 8000 groups are selected as a training set and the rest 9600 groups are selected as a test set.

Secondly, in order to facilitate the solution of neural network, the data need to be normalized. The following formula (8) is used for processing:

$$x_i = \frac{x_i - \bar{x}_i}{\sigma_i} \quad i=1 \sim 4 \quad (8)$$

Where  $x_i$  is the  $i$ -th feature of input variables,  $\sigma_i$  is the variance of  $x_i$ .

Thirdly, the recurrent neural network will be trained by the training set. As a fully interconnected network, there are four neurons in the input layer, one neuron in the output layer, five neurons in the forgetting gate, the input gate and the output gate respectively as the hidden layers. The biases of the three gates are three random numbers.

At last, the weight of each neuron connection is optimized by the AdaGrad Optimization method (Duchi, Hazan, and Singer, 2011), so that the output data is fitted to the field data.

The trained model is tested by the test set, and the results of test are shown in the following Figs. 7-8:

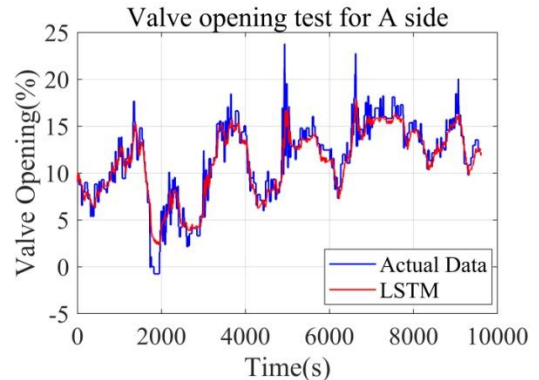


Fig. 7. Valve opening comparison for A side.

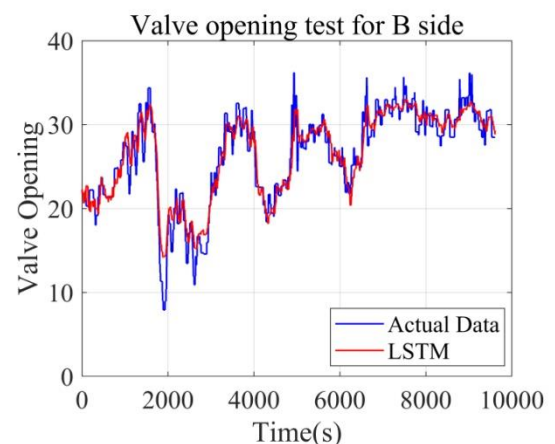


Fig. 8. Valve opening comparison for B side.

On one hand, as seen from Figs. 7-8, most of the points can approximately fit the field data. On the other hand, it also indicates that the recurrent neural network may have over-fitting problems, and the generalization ability needs to be further improved.

### 3.3.2 Model Predictive Control

Because of the unknown disturbances caused by the change of steam flow, the heat change of flue gas and flow change of desuperheating water, MPC can predict the future inputs within a certain range avoiding over-fitting. Thus, this paper introduces MPC control in the control strategy to solve the over-fitting problem of LSTM. According to the filed closed-loop data, the models of the two desuperheaters and the secondary superheater are respectively identified by using Prediction Error Method to establish prediction models. The transfer functions of models for two desuperheaters are shown as

$$y = \frac{-3.799 \cdot 10^{-4}}{z-0.9910} * u_1 + \frac{-0.0085}{z-0.9910} * u_2 + \frac{0.0051}{z-0.9910} * u_3 \quad (9)$$

$$y = \frac{-1.929 \cdot 10^{-6}}{z-0.9947} * u_1 + \frac{-0.0025}{z-0.9947} * u_2 + \frac{0.0037}{z-0.9947} * u_3 \quad (10)$$

where  $y$  is the outlet steam temperature of the A and B side desuperheaters;  $u_1$  is the main steam flow;  $u_2$  is the valve opening;  $u_3$  is the inlet steam temperature of desuperheater. The transfer function of the models for the secondary superheater is shown as

$$y = \frac{0.0011}{z-0.9963} * u_1 + \frac{0.0119}{z-0.9963} * u_2 + \frac{1.3 \cdot 10^{-4}}{z-0.9963} * u_3 + \frac{5.598 \cdot 10^{-5}}{z-0.9963} * u_4 \quad (11)$$

where  $y$  is outlet steam temperature of the secondary superheater;  $u_1$  is outlet steam temperature of the desuperheater of A side;  $u_2$  is outlet steam temperature of the desuperheater of B side;  $u_3$  is the steam flow of A side;  $u_4$  is the steam flow of B side.

According the transfer functions, the state-space expressions of the prediction model is established as formula (12). The valve openings of A and B side are taken as the input, and the outlet temperature of the secondary superheater is taken as the output.

$$A = \begin{bmatrix} 0.9161 & 0.1780 & -0.1629 \\ -0.4133 & 1.9748 & -0.9003 \\ -0.4148 & 0.9838 & 0.0911 \end{bmatrix} \quad B = \begin{bmatrix} -0.0026 & 0.0003 \\ 0.0008 & 0.0038 \\ 0.0008 & -0.0001 \end{bmatrix} \quad (12)$$

$$C = [-0.0024 \quad 0.0000 \quad -0.0076] \quad D = [0 \quad 0]$$

Designing an optimization function shown as the formula (13) and considering the valve opening on the A and B sides as the constraints shown as the formula (14):

$$J = (Y_r - Y_k) * Q * (Y_r - Y_k) + \Delta U * R * \Delta U \quad (13)$$

$$\begin{bmatrix} 0 \\ 0 \end{bmatrix} \leq u \leq \begin{bmatrix} 80 \\ 80 \end{bmatrix} \quad (14)$$

where  $Y_r$  is the set-point of output;  $Y_k$  is the field output;  $Q$  is the error weight;  $R$  is the control weight;  $\Delta U$  is the input increment.

The objective function is transformed into the standard quadratic form and the optimization problem is solved by combining the constraints. The set-point of superheated steam temperature is 543 °C, the prediction horizon is 30 s, and the control horizon is 5 s.

### 3.3.3 Weight Optimization

Particle swarm optimization algorithm has been widely used in various fields of life. In order to find the optimal ratio of model predictive control and recurrent neural network control, two control methods are weighted by particle swarm optimization in this paper. The initial value of two weights is [0.5, 0.5], the number of initial population is 30 and the maximum iteration is 15. The speed of particles is limited to [0, 0.1]. ITAE index is used as cost function of PSO. The optimization range is between [0, 1].

After optimization, MPC control on A side accounted for 60%, and MPC control on B side accounted for 53.8%.

## 4. ANALYSIS OF LSTM-MPC CONTROL

According to the above control strategy, the secondary superheated steam temperature control is simulated in SIMULINK and compared with the actual PID control and single MPC control. Parameters of outer loop of PID are  $k_p=0.6$ ,  $k_i=0.005$ . Parameters of inner loop of A and B sides are  $k_{pa}=2.4$ ,  $k_{ia}=0.004$ ,  $k_{pb}=2.5$ ,  $k_{ib}=0.0083$ . The parameters of single MPC are that the prediction horizon is 30 s, and the control horizon is 5 s. Comparison between LSTM-MPC and PID control is shown in Figs. 9-10.

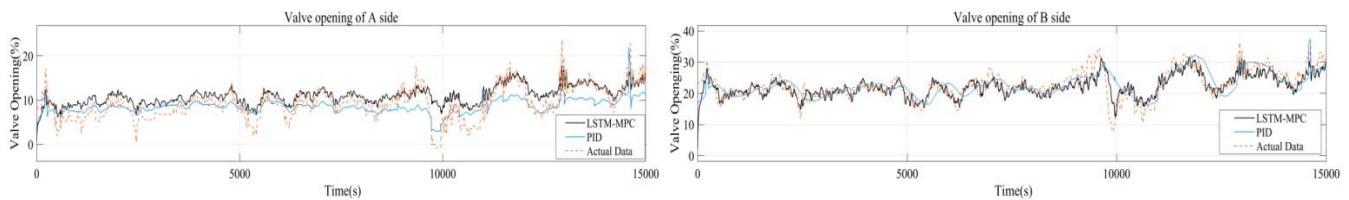


Fig. 9. Valve opening of A and B sides.

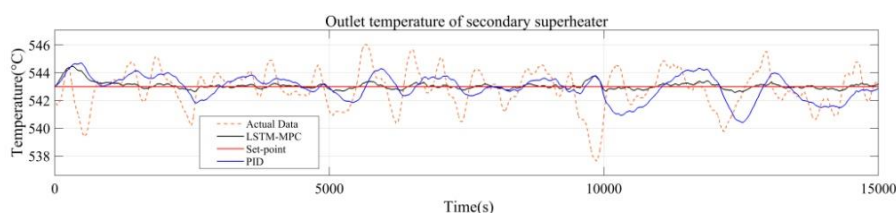


Fig. 10. Outlet temperature of secondary superheater.

As can be seen from Figs. 9-10, compared with the traditional PID control, the LSTM-MPC can significantly improve the outlet steam temperature of the secondary superheater. At the same time, it can better match the set-point, and the fluctuation is less. The valve opening of A

and B side has more small fluctuations, which is more consistent with the actual situation.

Comparison between LSTM-MPC and single MPC control is shown in Figs. 11-12.

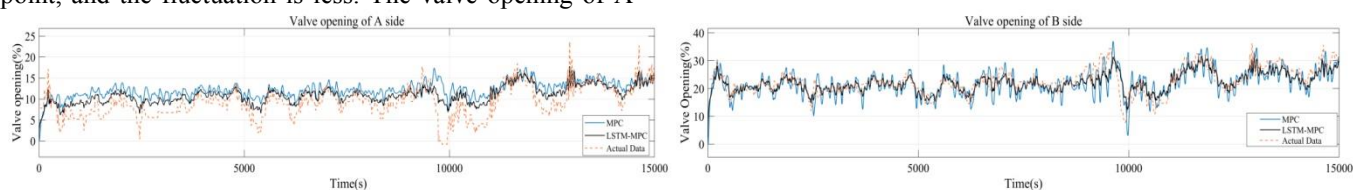


Fig. 11. Valve opening of A and B sides.

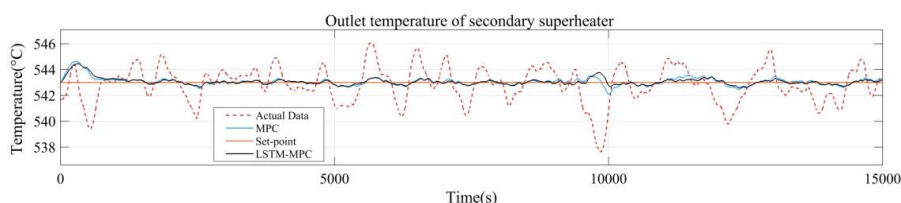


Fig. 12. Outlet temperature of secondary superheater.

As can be seen from Figs. 11-12, when using single MPC control, the valve opening fluctuates greatly, especially on side B. However, the LSTM-MPC can reduce the fluctuation of the valve and make the valve opening reach the practical state under the premise of ensuring the stability of the outlet temperature of secondary superheater.

## 5. CONCLUSION

In order to improve the accuracy of superheated steam temperature and the stability of valves for desuperheating water, we propose a control strategy (LSTM-MPC) combined by LSTM and MPC and weighted by PSO. The LSTM is used to learn potential characteristics in data and MPC is used to control the outlet temperature of secondary superheater. From the simulation results of this paper, the variability of the desuperheater valve is significantly reduced, and the outlet steam temperature of secondary superheater is closer to the set-point.

## ACKNOWLEDGEMENT

This work was supported by the National Natural Science Foundation of China under Grant 51936003.

## REFERENCE

Ren, C., (2019). "Application of EMD-LSTM Algorithm in Short-Term Power Load Forecasting." *Electric Power Science and Engineering* 8.

Geng, P., (2019). "Battery SOC prediction method based on LSTM cyclic neural network." *Journal of Shanghai Maritime University* 40.3: 120-126.

Chen, Z, Q., Cheng, J., (2019). "Fault diagnosis based on deep confidence network wind turbine pitch system." *Measurement and Control Technology* 38.05:23-27.

Zhou, Z., (2016). "Carbon risk warning research on heavily polluting industrial enterprises based on support vector machine." *Environmental Pollution and Prevention* 38.1.

Xi, C., (2016). Nonlinear predictive control based on Hammerstein model. *Diss.*

Cao, S. (2019). "Load Control of Wind Turbines Based on Model Predictive Control." *Journal of Suzhou University of Science and Technology (Natural Science Edition)* 36.3.

Xiao, H., Fei, P., and Li, K., (2016). "Multi-time scale coordinated optimization scheduling of microgrid based on model predictive control." *Power System Automation* 40.18: 7-14.

Rao, G., Huang, W., Feng, Z., (2018). "LSTM with sentence representations for document-level sentiment classification." *Neurocomputing*, 308:49e57.

Duchi, J., Hazan, E., and Singer, Y., (2011). Adaptive Subgradient Methods for Online Learning and Stochastic Optimization. *JMLR.org*.